

**N75-33289**

## REQUIREMENTS FOR SPACE SHUTTLE SCATTER RADAR EXPERIMENTS

by

K. J. Harker

NASA Grant NGL 05-020-176

(CR-119091 REQUIREMENTS FOR SPACE SHUTTLE SCATTER  
RADAR EXPERIMENTS (Stanford Univ.) 32p HC \$3.75  
CSCL L71

N75-33289

Unclas  
GE/32 42276

SU-IPR Report No. 643

October 1975

[Material to be presented at URSI Meeting,  
Boulder, Colorado, October, 1975]

Institute for Plasma Research  
Stanford University  
Stanford, California 94305

REQUIREMENTS FOR SPACE SHUTTLE SCATTER RADAR EXPERIMENTS

by

K. J. Harker

Institute for Plasma Research  
Stanford University  
Stanford, California 94305

ABSTRACT

The feasibility of carrying out scatter radar experiments on the Space Shuttle has been analyzed. Design criteria considered were the required average transmitter power, frequency resolution, spatial resolution, and statistical accuracy. Experiments analyzed were measurement of the naturally enhanced plasma line and the ion component of the incoherent scatter spectrum, and the plasma line artificially enhanced by an intense HF radio wave. The ion component measurement does not appear feasible, while the other two appear reasonable for short ranges only.

## 1. Introduction

Recently there has been considerable interest in the possibility of using scatter radar aboard the Space Shuttle. The reason for this stems mainly from the fact that the strength of a radar signal is inversely proportional to the range. Results equivalent to those with a ground-based transmitter should be obtainable with a transmitter of much lower power.

The purpose of this paper will be to evaluate the practicality of scatter radar on board the Shuttle. As one might expect, this raises a whole new set of problems whose disadvantages must be carefully weighed against the advantages of close proximity to the region being probed. Among these are the limited power available, the limited time available for measurement due to the motion of the Shuttle, and the interference from ground clutter.

Our evaluation will be carried out by examining in detail three types of experiments: measurement of the plasma line of the incoherent scatter spectrum, measurement of the ion line, and measurement of the plasma line enhanced by an intense HF radio wave. In each case we will consider an idealized optimized measurement system in order to obtain as favorable an evaluation as possible. The variables to be evaluated are the average radar transmitter power, the HF power (in the case of the modification experiment), the spatial resolution, and the frequency resolution.

## 2. Scattered Power

In this section we derive expressions for the scattered power arriving at the receiver. Our starting point is the high-frequency expansion for incoherent scatter given by Harker and Crawford [1974, Eq. (78)]

$$\frac{\partial^2 P}{\partial \Omega \partial \omega_\alpha} = \frac{r_0^2 S_\beta V N S(\underline{k}_\gamma, \omega_\gamma)}{2\pi} \quad (1)$$

where

$$S(\underline{k}_\gamma, \omega_\gamma) = \frac{4\pi}{N} \left\{ |1 + \chi_{i\gamma}|^2 \int_{-\infty}^{\infty} f_{0e}(v) \delta(\omega_\gamma - \underline{k}_\gamma \cdot \underline{v}) dv \right. \\ \left. + |\chi_{e\gamma}|^2 \int_{-\infty}^{\infty} f_{0i}(v) \delta(\omega_\gamma - \underline{k}_\gamma \cdot \underline{v}) dv \right\}, \quad (2)$$

$r_0$  is the classical electron radius,  $S_\beta$  is the incident power flux in the scattering region,  $V$  is the volume,  $N$  is the number density,  $S(\underline{k}_\gamma, \omega_\gamma)$  is the spectral density,  $\chi_{e\gamma}$  and  $\chi_{i\gamma}$  are the electron and ion susceptibilities,  $f_{0e}$  and  $f_{0i}$  are the electron and ion number densities,  $\Omega$  is the solid angle subtended by the antenna,  $\omega_\alpha$  is the (positive) radian frequency of the scattered wave, and  $P$  is the scattered power at the receiver. Because of the geometrical relationships

$$V = A_s \Delta h \quad d\Omega = A_r / h^2 \quad P_T = S_\beta A_s \quad (3)$$

where  $A_s$  and  $\Delta h$  are the horizontal area and thickness of the scattering region,  $A_r (= \eta_A \pi r_A^2)$  is the antenna aperture,  $r_A$  is the antenna radius,  $\eta_A$  is the antenna efficiency,  $h$  is the range, and  $P_T$  is the incident power, we may rewrite (1) as

$$\frac{\partial P}{\partial \omega_\alpha} = \frac{r_0^2 N P_{Tr} A S(\underline{k}_\gamma, \omega_\gamma) \Delta h}{2\pi h^2} \quad (4)$$

For the natural plasma line and auto-correlation measurements we desire the integral of (4) over all frequencies. This is done by evaluating

$$S(\underline{k}_\gamma) = \int_0^\infty S(\underline{k}_\gamma, \omega_\gamma) d\omega_\gamma \quad (5)$$

and the results are [Ichimaru, 1973]

$$S(\underline{k}_\gamma) = \pi \quad P = r_0^2 N P_{Tr} A \Delta h / (2h^2) \quad \text{ion component} \quad (6)$$

$$S(\underline{k}_\gamma) = 2\pi(k_\gamma \lambda_D)^2 \quad P = r_0^2 N P_{Tr} A (k_\gamma \lambda_D)^2 \Delta h / h^2 \quad \text{plasma line .}$$

In the case of HF induced enhancements, the starting point is the equation for scattering by strongly driven plasma waves [Harker and Crawford, 1974, Eq. 81]:

$$\frac{\partial^2 P}{\partial \omega_\alpha \partial \omega_\alpha} = \frac{r_0^2 S_\beta v}{\pi} \frac{k_\gamma^2 \epsilon_0^2}{e^2} |x_{e\gamma}|^2 \lim_{T, V \rightarrow \infty} \frac{|E_\gamma|^2}{TV} \quad (7)$$

In this formula  $T$  is the observation time and  $V$  is some local sub-volume of the total scattering volume. Substituting (3) and the relations

$$\frac{\epsilon_0}{e^2} = \frac{\lambda_D^2 N}{K_B T} \quad V = A_s \int dh = 2 A_s H_s \int \frac{d\omega_p}{\omega_p} \quad (8)$$

$$x_{e\gamma} \approx 1$$

where  $\lambda_D$  is the Debye wavelength,  $K_B$  is Boltzmann's constant,  $T$  is the ionospheric temperature,  $H_s$  is the scale height, and  $\omega_p$  is the local electron plasma frequency, we obtain

$$\frac{\partial p}{\partial \omega_\alpha} = \frac{2r_0^2 H_s N(k_Y \lambda_D)^2 P_{T r}^A}{\pi h^2} \int \frac{d\omega_p}{\omega_p} \lim_{T, V \rightarrow \infty} \frac{1}{TV} \frac{\epsilon_0 |E_Y|^2}{K_B T} . \quad (9)$$

If we invoke the random phase approximation, we may approximate  $|E_Y|^2$  by

$$|E_Y|^2 = |\hat{E}(\underline{k}_Y)|^2 \delta[\omega_\alpha - \omega_\beta - \omega_Y(\underline{k}_Y)] \quad (10)$$

where

$$\underline{k}_Y = \frac{\underline{r}}{|\underline{r}|} k_\alpha(\omega_\alpha) - \underline{k}_\beta \quad (11)$$

and  $\underline{r}$  is the vector pointing from the scattering region to the radar receiver. Since  $Y$  refers to a plasma wave, it can be shown that  $d\omega_p \approx d\omega_Y$ . We may replace  $d\omega_p$  by  $d\omega_Y$  in (9) and integrate over the delta-function to obtain

$$\frac{\partial p}{\partial \omega_\alpha} = \frac{2r_0^2 H_s N(k_Y \lambda_D)^2 P_{T r}^A}{\pi h^2 \omega_p} \lim_{T, V \rightarrow \infty} \frac{1}{TV} \frac{\epsilon_0 |\hat{E}(\underline{k}_Y)|^2}{K_B T} \quad (12)$$

and the condition

$$\omega_\alpha - \omega_\beta - \omega_Y(\underline{k}_Y) = 0 . \quad (13)$$

Let us introduce the quantity  $I$  through the relation

$$I = 4 \lim_{T, V \rightarrow \infty} \frac{1}{TV} \epsilon_0 |\hat{E}(\underline{k}_Y)|^2 . \quad (14)$$

Then (12) can be written simply as

$$\frac{\partial p}{\partial \omega_\alpha} = \frac{r_0^2 H_s N(k_Y \lambda_D)^2 P_{T r}^A}{2\pi h^2 \omega_p} \left( \frac{I}{K_B T} \right) . \quad (15)$$

DuBois and Goldman [1972, Eq. (8)] have shown that  $I$  is given by the relation

$$\frac{I}{K_B T} = \frac{4\pi E^2 S}{\alpha k_Y \lambda_D} \frac{\mu^2}{1-\mu^2} \frac{1}{1+X^2} \quad (16)$$

where

$$E^2 S = \frac{\epsilon_0}{16NK_B T} \frac{\omega}{\gamma_e} E_0^2 S \quad (17)$$

is the ratio of the HF wave power flux to the threshold flux,

$$S = 2 \left[ \left( \frac{\omega_c}{\omega_0} \right)^2 (1-\mu^2) + 3k_Y^2 \lambda_D^2 \right]^{-1/2} \quad (18)$$

is the swelling factor [Ginzburg, 1964],

$$X = \frac{\omega_0 - \omega_Y(k_Y) - \alpha k_Y v_e}{\alpha k_Y v_e} , \quad (19)$$

$\alpha$  is the square root of the electron to ion mass ratio,  $v_e$  is the electron thermal velocity,  $\omega_0$  is the HF wave frequency,  $\omega_c$  is the electron cyclotron frequency,  $\mu$  is the sine of the dip angle, and  $E_0$  is the HF electric field that would be present if there were no plasma. From elementary antenna theory we know that

$$E_0^2 = \frac{P_0 G}{2\epsilon_0 \pi c h^2} \quad (20)$$

where  $G$  is the antenna gain and  $P_0$  is the transmitter power. For a Yagi-type HF antenna,  $G = 5$ , while for a parabolic antenna we have

$$G = \frac{4\pi A \eta_A}{c^2} f^2 \quad (21)$$

where  $\eta_A$  is the antenna efficiency.

If we wish to obtain the total power scattered, we must integrate (15) over  $\omega_\alpha$ . The only factor of significant variation is the

$(1 + X^2)^{-1}$  in (16), so we need to find

$$\int_0^{\infty} \frac{1}{1+X^2} d\omega_{\alpha} \quad (22)$$

Noting from (13) and (19) that we may replace  $d\omega_{\alpha}$  by  $\alpha k_{\gamma} v_e X$ , we readily determine that this integral is equal to  $\frac{\pi \alpha k_{\gamma} v_e}{2}$ . This gives a total power returned of

$$P = \frac{\pi r_0^2 H_s N(k_{\gamma} \lambda_D)^2 P_{Tr} E^2 S}{h^2} \frac{\mu^2}{1-\mu^2} \quad (23)$$



### 3. Statistical Accuracy

In order to evaluate the feasibility of the scatter radar system, it is important to know the statistical accuracy with which the scattered signal can be determined. This is determined by a number of factors, including signal-to-noise ratio, pulse length, number of pulses, and receiver bandwidth. One must also distinguish between methods for resolving the spectrum as a function of frequency. One method of doing this is by measuring the auto-correlation function, and then numerically transforming to the frequency domain. This measurement can be carried out by transmitting groups of pulses and measuring the return. If there are  $K$  groups of pulses with  $n_p$  pulses per group, then it can be shown [Farley, 1972] that the rms error,  $\epsilon$ , of each lag-product in the correlation function is given by

$$\epsilon^2 = \frac{1}{K} \left( n_p + \frac{P_N}{P} \right)^2 \quad (24)$$

where  $P$  is the signal power and  $P_N$  is the noise power, given by

$$P_N = K_B T_N \Delta f . \quad (25)$$

Another way of resolving the spectrum is to pass the received signal through a filter bank and determine the spectrum as a function of frequency directly. The rms error of each frequency component is then given by

$$\epsilon^2 = \frac{1}{K\tau\Delta f} \left( 1 + 2 \frac{P_N}{P} \right) \quad (26)$$

where  $K$  is the total number of pulses,  $\tau$  is the pulse length,  $\Delta f$  is the bandwidth of each filter in the bank, and  $P_N$  is again given by (25).

1. The first part of the document discusses the importance of maintaining accurate records of all transactions and activities. It emphasizes that this is crucial for ensuring transparency and accountability in the organization's operations.

2. The second part of the document outlines the various methods and tools used to collect and analyze data. It highlights the need for consistent and reliable data collection processes to support effective decision-making.

3. The third part of the document focuses on the role of technology in data management and analysis. It discusses how modern software solutions can streamline data collection, storage, and reporting, thereby improving efficiency and accuracy.

4. The fourth part of the document addresses the challenges associated with data management, such as data quality, security, and privacy. It provides strategies to mitigate these risks and ensure that data is used responsibly and ethically.

5. The fifth part of the document concludes by summarizing the key findings and recommendations. It stresses the importance of ongoing monitoring and evaluation to ensure that data management practices remain effective and up-to-date.

6. The sixth part of the document provides a detailed overview of the data collection process, including the identification of data sources, the design of data collection instruments, and the implementation of data collection procedures.

7. The seventh part of the document discusses the various methods used for data analysis, such as descriptive statistics, inferential statistics, and regression analysis. It explains how these methods can be used to interpret the data and draw meaningful conclusions.

8. The eighth part of the document focuses on the importance of data visualization in presenting the results of data analysis. It discusses various visualization techniques, such as bar charts, line graphs, and pie charts, and their effectiveness in communicating complex data.

9. The ninth part of the document addresses the ethical considerations surrounding data management and analysis. It discusses the need for transparency, informed consent, and data protection to ensure that the use of data is fair and just.

10. The tenth part of the document provides a final summary and conclusion, reiterating the key points and emphasizing the importance of data management and analysis in achieving organizational success.

11. The eleventh part of the document discusses the role of data in strategic planning and decision-making. It explains how data can provide valuable insights into market trends, customer behavior, and operational performance, which can be used to inform strategic decisions.

12. The twelfth part of the document focuses on the importance of data security and privacy in the digital age. It discusses the various threats to data security and the measures that can be taken to protect sensitive information from unauthorized access and disclosure.

13. The thirteenth part of the document discusses the role of data in innovation and research. It explains how data can be used to identify new opportunities, test hypotheses, and develop new products and services, thereby driving innovation and growth.

14. The fourteenth part of the document provides a final summary and conclusion, reiterating the key points and emphasizing the importance of data management and analysis in achieving organizational success.

15. The fifteenth part of the document discusses the future of data management and analysis. It explores emerging trends, such as big data, artificial intelligence, and cloud computing, and their potential impact on the way we collect, manage, and analyze data.

It should be pointed out that both (24) and (26) are based on the premise of noise cancellation. That is, it is assumed that the receiver power is measured in the absence of the signal, and this result is then subtracted from the receiver power measured in the presence of the signal.

Referring to (24), it is clear that one approaches the point of diminishing returns as the signal to noise ratio assumes values in the region of  $1/n_p$ . Beyond this point  $\epsilon$  can be effectively lowered only by increasing  $K$ . Therefore, when the correlation function method is used, we will assume that

$$P = \frac{P_N}{n_p} \quad \epsilon^2 = \frac{4n_p^2}{K} \quad (27)$$

Likewise, when we use the filter bank method and (26) applies, we shall assume that

$$P = 2P_N \quad \epsilon^2 = \frac{2}{KT\Delta f} \quad (28)$$

#### 4. Ground Clutter

Figure 1 shows the geometry of the scatter radar system for a shuttle flying at an altitude  $h_g$ . If the region being probed is a distance  $h$  below the shuttle, then a transmitted pulse will return at  $t_h = 2h/c$ . Clutter generated by this pulse will swamp any received signal during the period from  $t_g$  to  $t_e$ ,

$$t_g = 2h_g/c \quad t_e = \frac{2h_e}{c} = \frac{2}{c} (h_g^2 + 2h_g R_e)^{1/2}, \quad (29)$$

corresponding to reflection over the region from directly below the shuttle out to the shuttle's horizon. In order, therefore, to avoid interference from ground clutter it is necessary to confine the transmission of any train of pulses to a period of length  $t_g - t_h$ , followed by a period of no transmission of length  $t_e - t_g + t_h$ .

## 5. Plasma Line

In the case of the naturally occurring plasma line, we do not generally want the frequency spectrum, but rather the integral of the spectrum with respect to frequency. If one desires a height resolution of  $\Delta h$ , then the associated pulse length,  $\tau$ , and receiver bandwidth,  $\Delta f$ , are related by

$$\tau = \frac{2\Delta h}{c} \quad \Delta f = \frac{\omega_p \Delta h}{4\pi H_s} \quad (30)$$

A convenient pulse scheme for accomplishing this measurement is shown in Figure 2. Groups of pulses are transmitted over a period of  $t_h$ , followed by a like period  $t_h$  during which the receiver gate is open. This prevents the receiver gate from being open when the transmitter is on. Each group of pulses consists of individual pulses chosen to be of length  $\tau$  for height discrimination. The region probed by each pulse is shown as shaded. Clutter between individual pulses is prevented by transmitting the individual pulses at a sequence of frequencies separated by more than the receiver bandwidth,  $\Delta f$ . As mentioned above, the receiver gate must be closed between  $t_g$  and  $t_e$  in order to avoid ground clutter. Therefore the total number of pulses,  $K_g$ , that may be transmitted during a period  $t_e$  is given by

$$K_g = \left( \frac{t_h}{\tau} \right) \left( \frac{t_g}{2t_h} \right) = \frac{h_g}{2\Delta h} \quad (31)$$

If the measurement is made while the shuttle traverses a distance  $\Delta x$  at a velocity  $v_s$ , then the total number of pulses is

$$K = K_g \left( \frac{\Delta x}{v_s t_e} \right) = K_g \left( \frac{c \Delta x}{2v_s h_e} \right). \quad (32)$$

Referring to Fig. 2, it is also clear that the average transmitter power,  $P_A$ , can be written in terms of the peak transmitter power,  $P_T$ , by means of the relation

$$\frac{P_A}{P_T} = \frac{K_g \tau}{t_e} = K_g \frac{\Delta h}{h_e}. \quad (33)$$

Substituting (32) into (28) shows that we may measure the plasma line to a horizontal spatial resolution of

$$\Delta x = \frac{2v_s t_e}{K_g \epsilon^2 (\Delta f \tau)}. \quad (34)$$

The formula for the average power required is obtained by combining (6), (28), and (33). The result is

$$P_A = 2K_B T_N \Delta f \frac{h^2 K_g}{R r_0^2 N A_r (k_Y \lambda_D)^2 h_e}. \quad (35)$$

A factor  $R$  has been placed in the denominator to account for the enhancement of the plasmaline above the thermal level.

Using the numerical values given in Table I, we calculate from (34) a horizontal spatial resolution for this measurement of  $\Delta x = 0.5$  km. The corresponding average powers for various ranges are plotted in Fig. 3. The horizontal resolution is quite acceptable. However, since the maximum possible average power available is about 4 kW [Crawford, 1975], it would not be possible to measure the plasma line for the parameters in Table I for ranges greater than 8 km. However, as examination of (26) and (32)

shows, if we degrade the horizontal spatial resolution,  $\Delta x$ , sixfold, from 0.5 to 3 km, then the average power requirement,  $P_A$ , is reduced by a factor of eleven, and it should be possible to increase the range of the measurements to 25 km.

## 6. Ion Component

In the case of the ion component, it is necessary to determine the spectrum as a function of frequency to a resolution of about 1-5 kHz. We cannot use the method of the previous section, therefore, and must use either a bank of filters or a correlation function technique. The former method is not feasible, since the vertical range discrimination will require a pulse too short to satisfy the criterion that  $\tau \Delta f$  be greater than unity. We are left, therefore, with the correlation function technique as our only alternative.

Farley [1972] has described possible pulse schemes for correlation measurements which eliminate clutter between adjoining pulses. The most suitable one for our purposes has five pulses (corresponding to  $n_p = 5$  in (24)) occurring at 0, 3, 4, 9, and 11  $t_c$ , where  $t_c$  is some basic time unit. The intervals between the pulses are 3, 1, 5, and 2  $t_c$  and all lags between 1 and 11  $t_c$ , except for 10  $t_c$ , may be determined. The length of each pulse,  $\tau$ , is chosen to give the desired vertical height discrimination, but certainly must be less than  $t_c$ . The length of the entire train is  $11 t_c + \tau \approx 12 t_c$  and must of course be chosen less than  $t_g$ . Such a system is able to analyze a spectrum of bandwidth equal to  $1/t_c$  to a resolution of  $1/12 t_c$ . If we choose  $t_c = \tau = 20 \mu\text{sec}$ , the height discrimination is 3 km, the frequency resolution is 5 kHz, and the signal bandwidth may be as wide as 50 kHz.

The total number of groups of pulses available in this method per period  $t_e$  is

$$K_g = \frac{t_g}{t_h + 12 t_e} \quad (36)$$

while the total number is

$$K = K_g \frac{\Delta x}{v_s t_e} \quad (37)$$



Substituting this into (27) and solving for  $\Delta x$  gives a horizontal spatial resolution of

$$\Delta x = \frac{4n_p^2 v_s t_e}{\epsilon^2} \left( \frac{t_h + 12 t_c}{t_g} \right). \quad (38)$$

The average power is related to the total power through the relations

$$P_A = \frac{n_p \tau}{t_e} \left( \frac{t_g}{t_h + 12 t_c} \right) P_T. \quad (39)$$

Combining this with (6), (27), and (39) shows that the required average power is given by

$$P_A = \frac{2h^2}{r_0^2 h_e NA_r \tau} \left( \frac{t_g}{t_h + 12 t_c} \right) K_B T_N. \quad (40)$$

Substituting the values in Table I into (38) and (40) shows that the horizontal spatial resolution and the average power vary as shown in Fig. 4. Note that the minimum range is 36 km. Both the horizontal spatial resolution and the average power are too large to allow the method to be useful, at least for the values in Table I.

## 7. Plasma Line with HF Induced Enhancement

When the ionosphere is irradiated with a strong HF radio wave, parametric interaction involving the decay of the incident ordinary HF electromagnetic wave into plasma waves and ion acoustic waves takes place. This gives rise to a plasma wave spectrum which is orders of magnitude above that occurring in natural incoherent scatter experiments. Because the phenomenon is not distributed vertically in space, but is, rather, confined to a narrow layer, height discrimination is relatively unimportant, and we may use the filter bank technique in addition to the correlation function method.

Combining (17) and (20), we find that the required HF transmitter power is given by

$$P_0 = \frac{32 \pi c h^2 N K_B T \gamma_e (E^2 S)}{G S \omega_0} \quad (41)$$

Since the inactive time between the scatter radar pulse train is roughly  $t_e - t_g = 11$  ms, and it takes roughly 100 ms for the parametric interaction process to saturate [Kantor, 1974], it is necessary to keep the HF power on continuously during the measurement. Therefore (41) also represents the average HF power required. This is plotted in Fig. 5 for various ranges. It is apparent from the plot that it will be practical to heat the ionosphere only for ranges less than 5 km.

Let us consider the correlation method first with the same pulsing scheme as in the previous section. A review of the arguments in the previous session show that (38) holds here also, and therefore the values for  $\Delta x$  in Fig. 4 again. Combining (23), (27), and (39), we find that

$$P_A = \frac{K_B T_N h^2}{\pi r_0^2 N A_r H_s (k_Y \lambda_D)^2 (E^2 S) t_e} \left( \frac{1-\mu^2}{\mu^2} \right) \left( \frac{t_g}{t_h + 12 t_c} \right) . \quad (42)$$

Both  $P_A$  and  $\Delta x$  are plotted in Fig. 6. The power demand is quite modest, but again, as in the case of the ion component, the poor horizontal spatial resolution length rules out the correlation method.

We turn finally to the filter bank method. A convenient pulsing scheme is shown in Fig. 7. The transmitter is turned on for time  $t_h$ , the receiver gate is opened for an equal time, and then the whole sequence repeats until  $t = t_g$ . The number of pulses that can be transmitted between 0 and  $t_e$  is

$$K_g = \frac{t_g}{2t_h} = \frac{h_g}{2h} . \quad (43)$$

The frequency resolution is  $\Delta f = 1/t_h$  and the total number of pulses is

$$K = \frac{h_g}{2h} \frac{\Delta x}{v_s t_e} . \quad (44)$$

The average power is given by

$$P_A = P_T \frac{K t_h}{t_e} = P_T \frac{h_g}{2h_e} . \quad (45)$$

Substituting (43) and (44) into (28) and solving for the horizontal resolution  $\Delta x$  gives

$$\Delta x = \frac{2 v_s t_e}{e^2 (h_g/2h)} . \quad (46)$$

Combining (15), (16), (28), and (45) with  $X = 1$  gives

$$P_A = \frac{K_B T_N (h_g / 2h_e) \omega_p h^2 \alpha}{2\pi r_0^2 N_A H_s (k_\gamma \lambda_D) (E^2 S)} \left( \frac{1-\mu^2}{\mu^2} \right). \quad (47)$$

In Fig. 8 have been plotted  $\Delta x$ ,  $\Delta f$ , and  $P_A$  as a function of range. The radar average pulse power requirement can be met out to about 60 km. In the region of short range, the horizontal spatial resolution is also very good, being of the order of 1 - 3 km. On the other hand, the frequency resolution is poor, of the order of 20 kHz. The frequency resolution greatly improves at larger ranges, but at the expense of horizontal resolution and impractically high radar and HF transmitter powers.

## 8. Summary

This study allows us to make the following conclusions regarding the feasibility of scatter radar measurements on the Space Shuttle when the radar beam is directed toward the earth, the vertical resolution is 3 km, 4 kW of average power is available, and the antenna radius is 10 m. The plasma line naturally enhanced by a factor of 50 can be measured out to a range of 25 km at a horizontal spatial resolution of 3 km. The ion line cannot be measured because the horizontal resolution is at best only 250 km. The same conclusion regards the HF wave enhanced plasma line when it is measured by the correlation function technique. It would be possible to measure the HF wave enhanced plasma line by the filter bank method out to a range of 5 km provided the poor frequency resolution of the order of 30 kHz were acceptable.

The radar transmitter power requirements for measuring the artificially enhanced plasma line could be greatly lessened by pointing the radar beam along the magnetic field lines instead of vertically downward, since the plasma wave spectrum is much stronger for waves propagating in this direction. In point of fact, however, little is really gained, because the main difficulty is with the frequency resolution and the HF power.

There are two ways in which it may be possible to substantially increase the power-aperture area products above the levels calculated in this paper. First, large furlable antennas may be available in the 1980's which have an aperture approximately 100 times greater than that of the 10 m radius antenna assumed in this paper. Second, megajoule capacitor banks may be available for the Shuttle in the near future. The energy requirement is determined for the various curves in this paper by forming the product  $P_A \Delta x / v_s$  and is always an increasing function

of the range. At a range of 100 km the radar energy requirement for the enhanced plasma line is 41 kJ; 3.7 MJ for the ion line; 170 kJ for the HF enhanced plasma line by the correlation function method, and 23 kJ by the filter bank method. The HF energy requirement is 2.5 MJ with the filter bank method and 87 MJ with the correlation function method. Therefore, the availability of such capacitor banks should bring most of the measurements described into the realm of possibility for ranges up to 100 km.

Finally, it should be pointed out that the spectrum  $S(\underline{k}_\gamma, \omega_\gamma)$  can be measured directly by a passive probe method. In this method the signal from two probes is passed through a cross-power spectrum analyzer [Harker and Ilić, 1974]. The cross-power spectrum so generated can then be Fourier transformed into  $S(\underline{k}_\gamma, \omega_\gamma)$ , provided measurements for a sufficient number of relative positions between the two probes have been taken. This procedure has been successfully carried out in the laboratory [Ilić and Harker, 1975; Ilić, Harker and Crawford, 1975]. Because this is an in situ measurement; because of the low power requirement, and because one obtains  $S(\underline{k}_\gamma, \omega_\gamma)$  for all values of  $\underline{k}_\gamma$  (instead of just the one obtained in the scatter radar case), we believe this method should be considered as a viable alternative to the scatter radar method.

#### ACKNOWLEDGMENTS

The author expresses his appreciation to F. W. Crawford for discussions and encouragement during this work; and M. Baron, J. Petriceks, and H. Kunnes for many useful discussions, particularly concerning the problem of ground clutter, frequency resolution, and statistical accuracy.

## REFERENCES

- Crawford, F. W. (1975), Plasma Wave and Resonance Phenomena, AIAA 13th Aerospace Sciences Meeting, Jan. 20-22, 1975, Pasadena, Calif., Paper 75-16.
- DuBois, D. F., and M. V. Goldman (1972) Spectrum and Anomalous Resistivity for the Saturated Parametric Instability, Phys. Rev. Lett. 28(4), 218-221.
- Farley, D. T. (1972), Multiple-pulse incoherent-scatter correlation function measurements, Radio Science 7(6), 661-666.
- Ginzburg, V. L. (1964), The Propagation of Electromagnetic Waves in Plasma, Pergamon, Oxford, pp. 193-195.
- Harker, K. J., and F. W. Crawford (1974), A theory for scattering by density fluctuations based on three-wave interaction, J. Plasma Phys. 11(3), 435-450.
- Harker, K. J., and D. B. Ilić (1974), Measurement of plasma-wave spectral density from the cross-power density spectrum, Rev. Sci. Instrum. 45(11), 1315-1324.
- S. Ichimaru (1973), Basic Principles of Plasma Physics, W. A. Benjamin, Inc., Reading, Mass, pp. 201 and 211.
- Ilić, D. B., and K. J. Harker (1975), Evaluation of plasma-wave spectral density from cross-power spectra, Rev. Sci. Instrum. 46(9), 1197-1200.
- Ilić, D. B., K. J. Harker, and F. W. Crawford (1975), Spectral Density of Ion Acoustic Plasma Turbulence, to be published in Phys. Letters.
- Kantor, I. J. (1974), High Frequency Induced Enhancements of the Incoherent Scatter Spectrum at Arecibo, 2, J. Geophys. Res. 79(1), 199-208.

Table I

$\alpha$	1/171
$r_0^2$	$7.94 \times 10^{-30} \text{ m}^2$
T	$1200^\circ \text{ K}$
$T_N$	$400^\circ \text{ K}$
$H_s$	$1 \times 10^5 \text{ m}$
N	$1 \times 10^{11} \text{ m}^{-3}$
$\omega_\beta/2\pi$	$6 \times 10^8 \text{ Hz}$
$\omega_c/2\pi$	$10^6 \text{ Hz}$
$\gamma_e$	650 Hz
$\cos^{-1} \mu$	$40^\circ$
$r_A$	10 m
$\eta_A$	0.4
$R_e$	$6.371 \times 10^6 \text{ m}$
$h_g$	$3 \times 10^5 \text{ m}$
$\epsilon$	0.1
$v_s$	$8 \times 10^3 \text{ m/s}$
$\Delta h$	$3 \times 10^3 \text{ m}$
$n_p$	5
$E^2 S$	2
G	5
R	50



## FIGURE CAPTIONS

- Figure 1: Ground clutter geometry. Clutter occurs for all ranges between  $h_g$  and  $h_e$ .
- Figure 2: Range-time diagram of the pulse pattern for measurement of the naturally enhanced plasma line.
- Figure 3: Average radar transmitter power as a function of range for measurement of the naturally enhanced plasma line,  $\Delta x = 0.5$  km.
- Figure 4: Average radar transmitter power and horizontal spatial resolution as a function of range for the ion component of the incoherent scatter spectrum.
- Figure 5: HF power as a function of range to give twice the threshold power flux required for parametric instability.
- Figure 6: Average radar transmitter power and horizontal spatial resolution as a function of range for measurement by the correlation method of the HF wave enhanced plasma line.
- Figure 7: Range-time diagram of the pulse pattern for measurement by the filter-bank method of the HF wave enhanced plasma line.
- Figure 8: Average radar transmitter power, horizontal spatial resolution, and frequency resolution as a function of range for measurement of the HF wave enhanced plasma line by the filter-bank method.

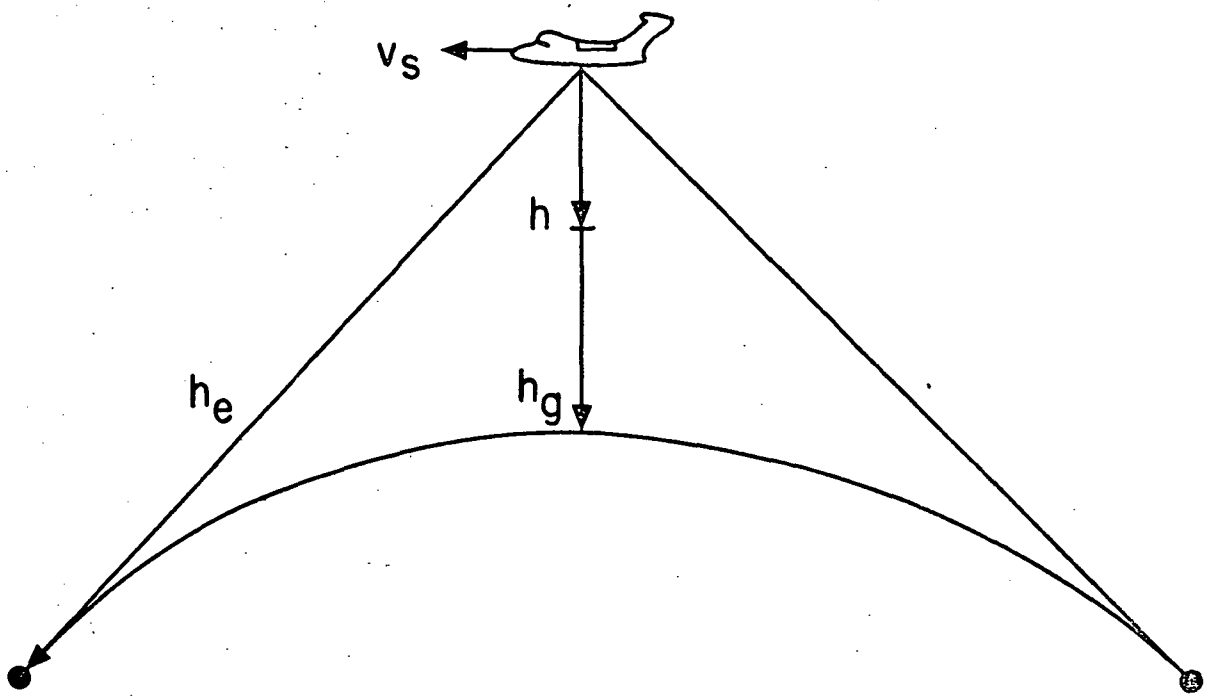


FIG. 1. Ground clutter geometry. Clutter occurs for all ranges between  $h_g$  and  $h_e$ .

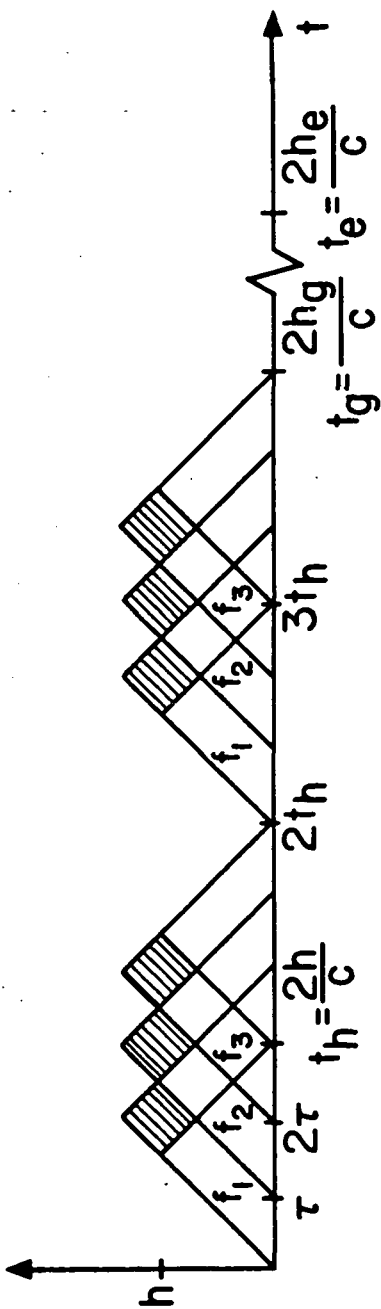


FIG. 2. Range-time diagram of the pulse pattern for measurement of the naturally enhanced plasma line.

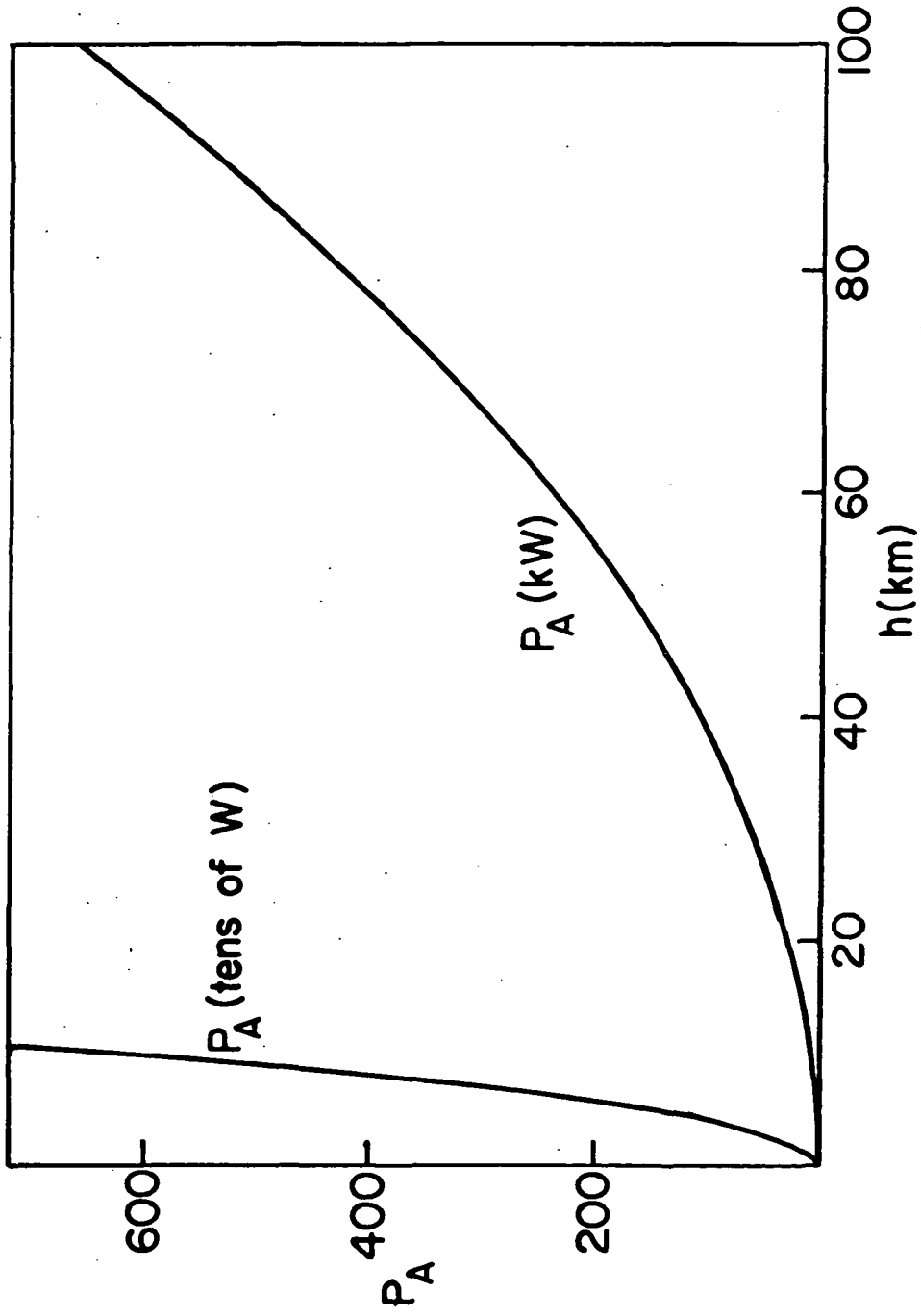


FIG. 3. Average radar transmitter power as a function of range for measurement of the naturally enhanced plasma line,  $\Delta x = 0.5$  km.

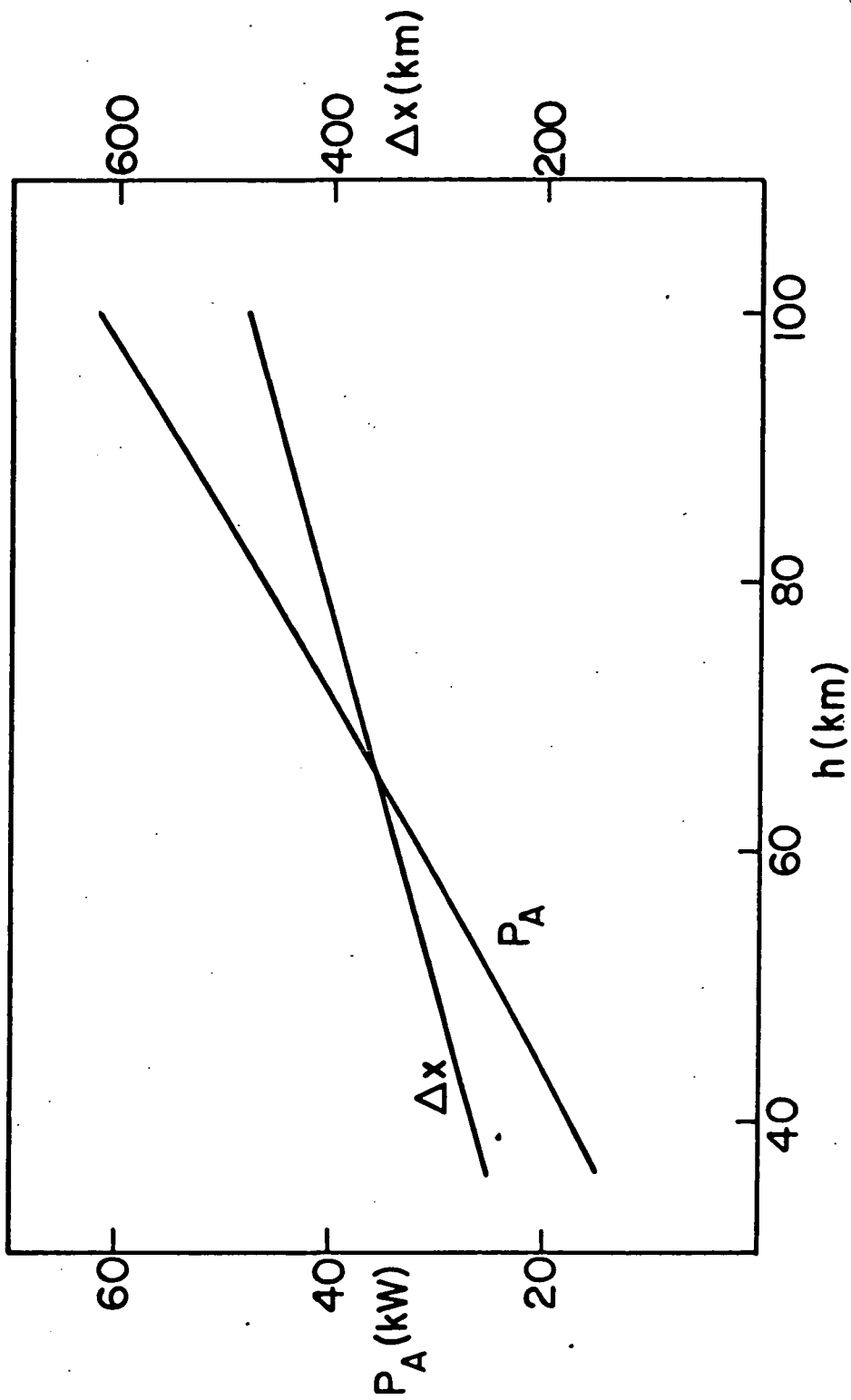


FIG. 4. Average radar transmitter power and horizontal spatial resolution as a function of range for the ion component of the incoherent scatter spectrum.

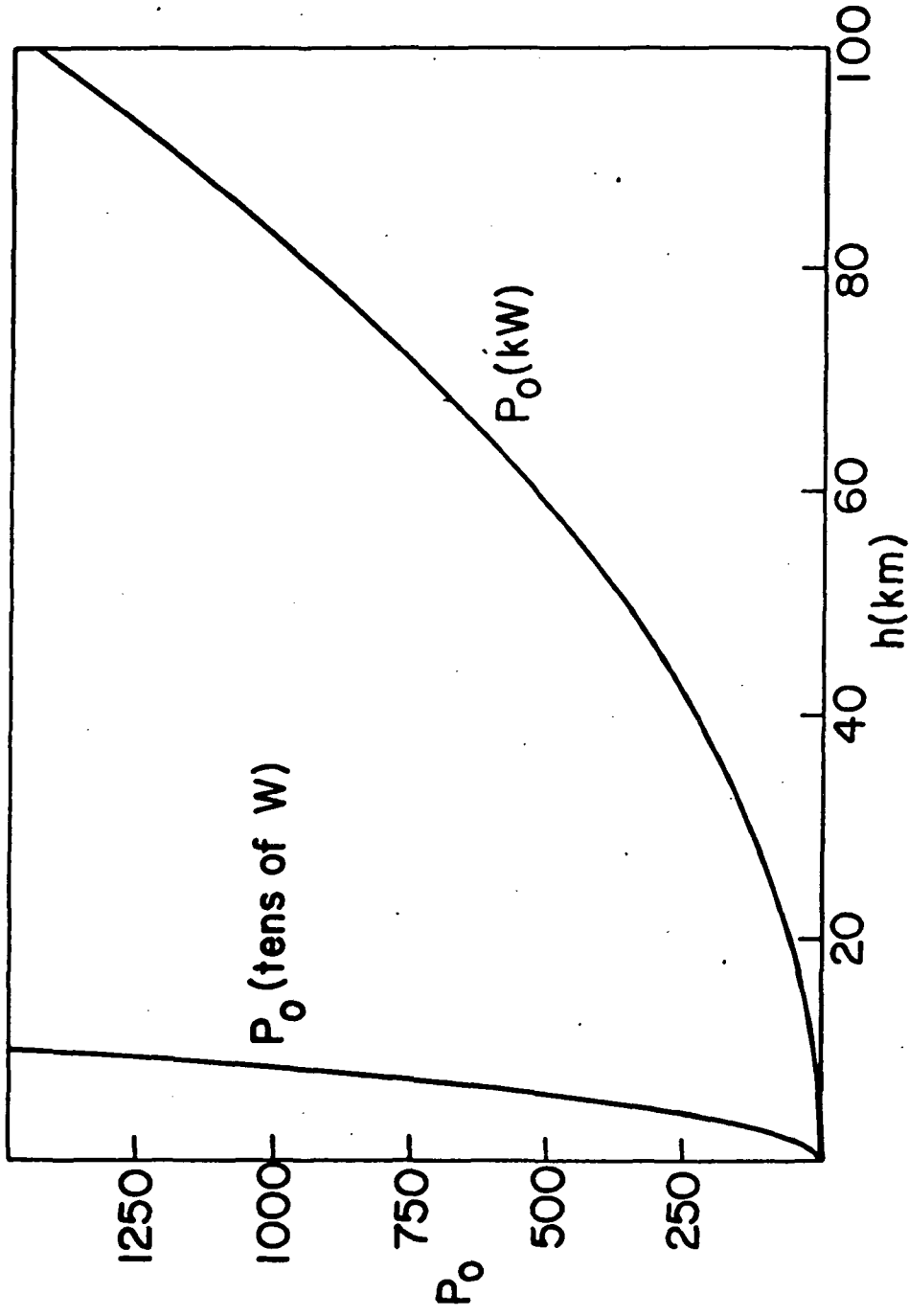


FIG. 5. HF power as a function of range to give twice the threshold power flux required for parametric instability.

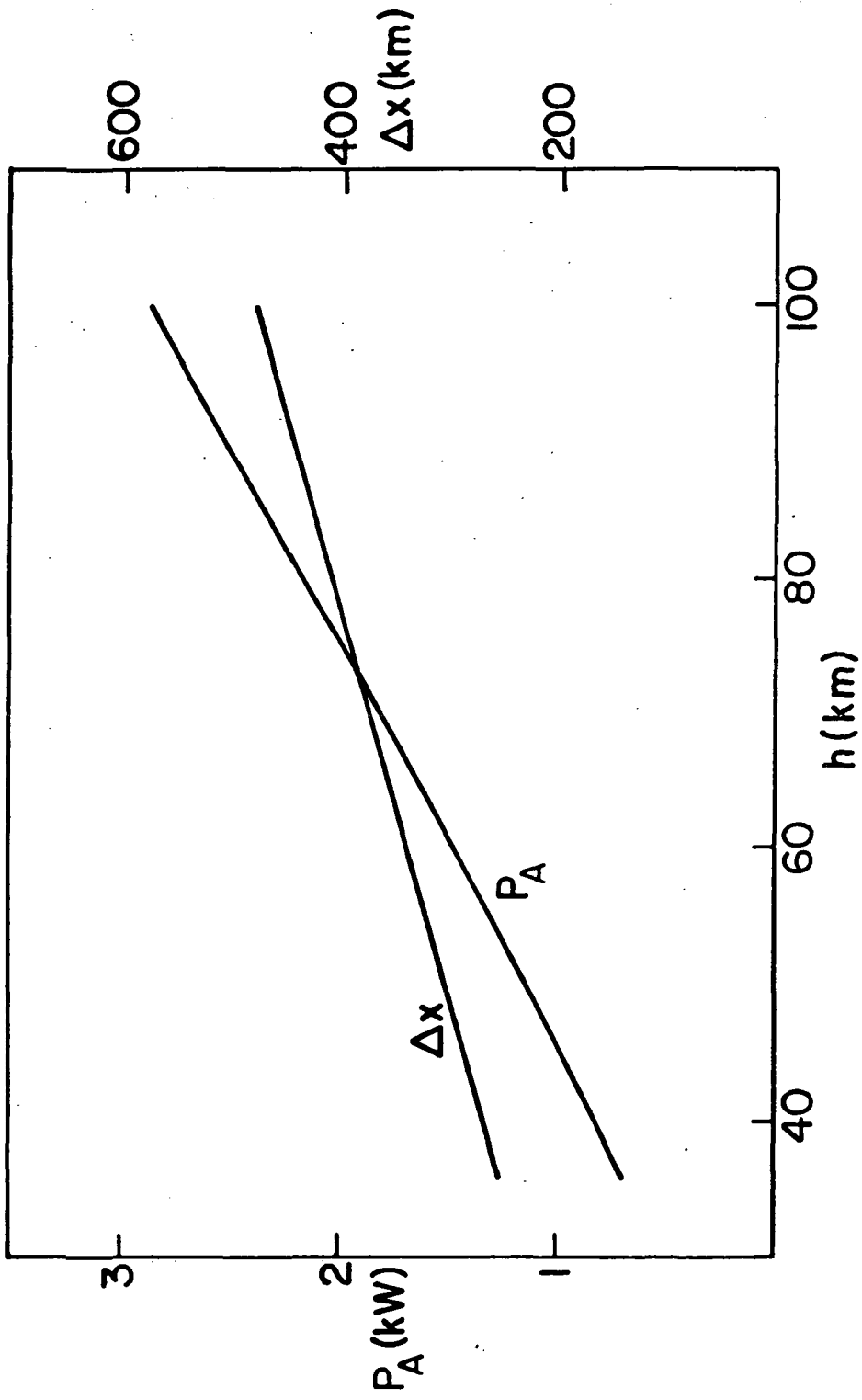


FIG. 6. Average radar transmitter power and horizontal spatial resolution as a function of range for measurement by the correlation method of the HF wave enhanced plasma line.

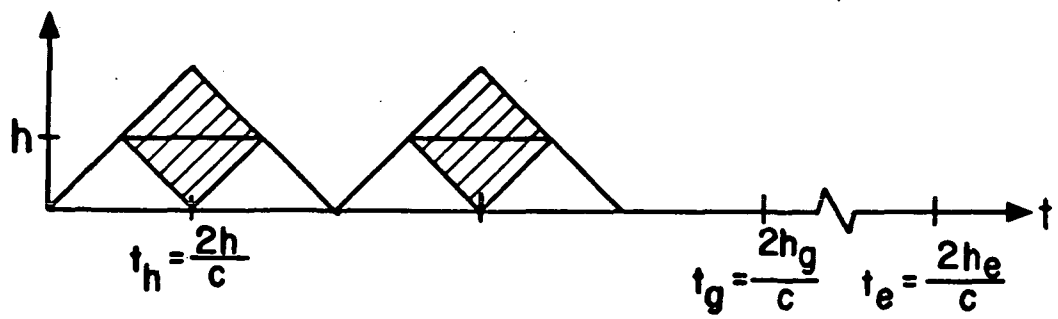


FIG. 7. Range-time diagram of the pulse pattern for measurement by the filter-bank method of the HF wave enhanced plasma line.



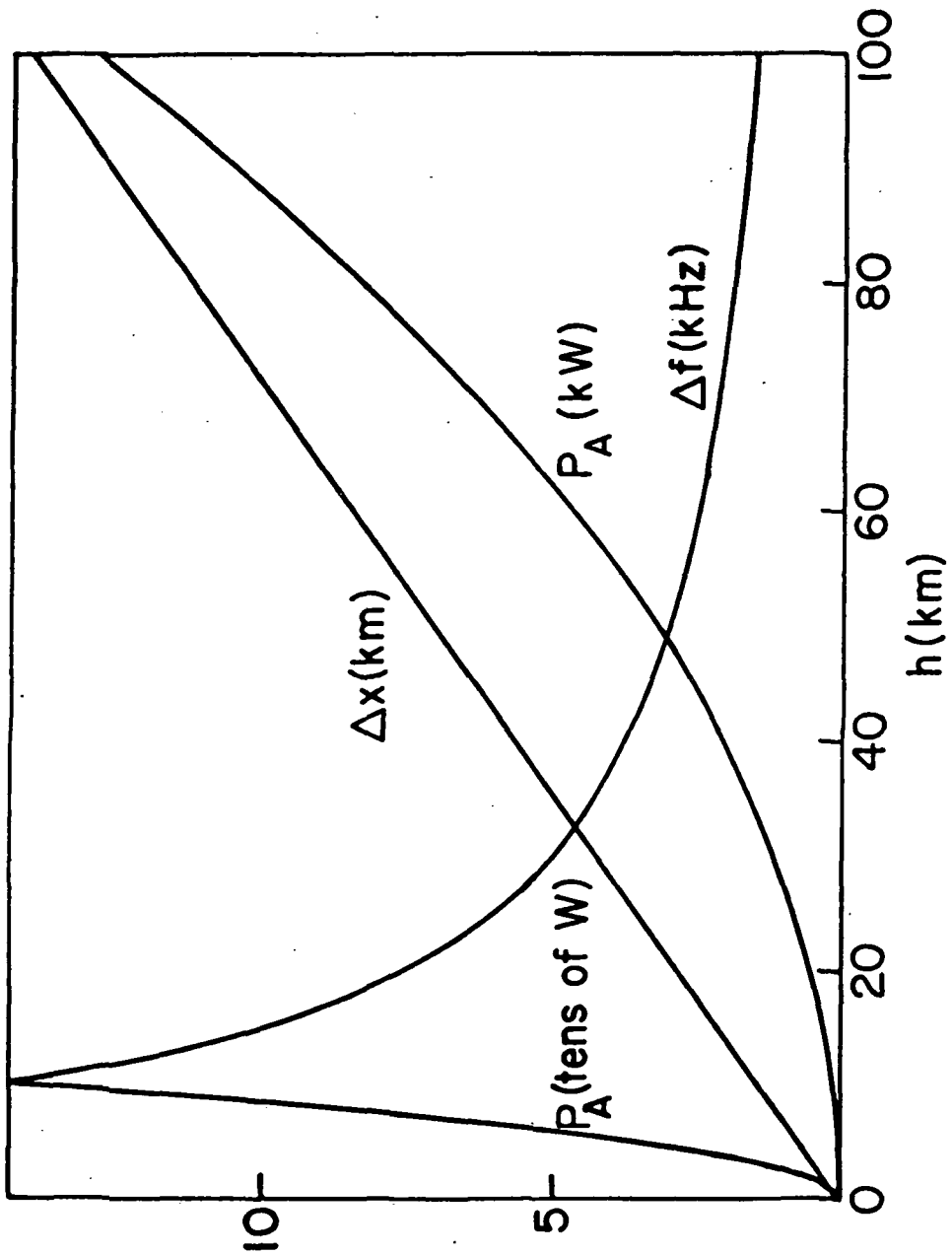


FIG. 8. Average radar transmitter power, horizontal spatial resolution, and frequency resolution as a function of range for measurement of the HF wave enhanced plasma line by the filter-bank method.

